



Published in final edited form as:

Cell. 2015 April 23; 161(3): 581–594. doi:10.1016/j.cell.2015.03.048.

Transbilayer Lipid Interactions Mediate Nanoclustering of Lipid-Anchored Proteins

Riya Raghupathy^{1,3,9}, Anupama Ambika Anilkumar^{1,3,9}, Anirban Polley^{2,8,9}, Parvinder Pal Singh⁶, Mahipal Yadav⁶, Charles Johnson⁵, Sharad Suryawanshi⁵, Varma Saikam⁶, Sanghapal D. Sawant⁶, Aniruddha Panda^{1,7}, Zhongwu Guo⁵, Ram A. Vishwakarma⁶, Madan Rao^{1,2,*}, and Satyajit Mayor^{1,4,*}

¹National Centre for Biological Sciences (TIFR), Bellary Road, Bangalore 560 065, India ²Raman Research Institute, C.V. Raman Avenue, Bangalore 560 080, India ³Shanmugha Arts, Science, Technology & Research Academy, Thanjavur 613401, India ⁴Institute for Stem Cell Biology and Regenerative Medicine, Bellary Road, Bangalore 560 065, India ⁵Wayne State University, 5101 Cass Avenue, Detroit, MI 48202, USA ⁶Indian Institute of Integrative Medicine (CSIR), Canal Road, Jammu 180001, India ⁷Manipal University, Madhav Nagar, Manipal 576104, Karnataka, India ⁸Tampere University of Technology, Korkeakoulunkatu 10, 33720 Tampere, Finland

SUMMARY

Understanding how functional lipid domains in live cell membranes are generated has posed a challenge. Here, we show that transbilayer interactions are necessary for the generation of cholesterol-dependent nanoclusters of GPI-anchored proteins mediated by membrane-adjacent dynamic actin filaments. We find that long saturated acyl-chains are required for forming GPI-anchor nanoclusters. Simultaneously, at the inner leaflet, long acyl-chain-containing phosphatidylserine (PS) is necessary for transbilayer coupling. All-atom molecular dynamics simulations of asymmetric multicomponent-membrane bilayers in a mixed phase provide evidence that immobilization of long saturated acyl-chain lipids at either leaflet stabilizes cholesterol-dependent transbilayer interactions forming local domains with characteristics similar to a liquid-ordered (lo) phase. This is verified by experiments wherein immobilization of long acyl-chain lipids at one leaflet effects transbilayer interactions of corresponding lipids at the opposite leaflet. This suggests a general mechanism for the generation and stabilization of nanoscale cholesterol-dependent and actin-mediated lipid clusters in live cell membranes.

*Correspondence: madan@ncbs.res.in (M.R.), mayor@ncbs.res.in (S.M.), <http://dx.doi.org/10.1016/j.cell.2015.03.048>.

⁹Co-first author

SUPPLEMENTAL INFORMATION

Supplemental Information includes Extended Experimental Procedures and seven figures and can be found with this article online at <http://dx.doi.org/10.1016/j.cell.2015.03.048>.

AUTHOR CONTRIBUTIONS

R.R., A.A.A., A.P., S.M., and M.R. designed the study. R.R. standardized the lipid incorporation methods, performed experiments, and analyzed the data involving the GPI analogs; A.A.A. performed experiments and analyzed the data involving the role of phosphatidylserine. A.P. performed the atomistic molecular dynamics simulations. P.P.S., M.Y., and C.J. prepared the GPI analogs, and S.S., V.S., and S.D.S. prepared the PS analogs. The design of the synthetic strategy and supervision was led by R.A.V. and Z.G. A.P. (NCBS) helped in performing the mass spectrometry experiments. R.R., A.A.A., A.P., M.R., and S.M. wrote the paper with input from all the authors.

INTRODUCTION

The plasma membrane of living cells is the barrier that segregates the inside of the cell from the outside. It is a fluid bilayer composed primarily of lipids and proteins. It has long been thought of as an equilibrium mixture giving rise to a “fluid mosaic” (Singer and Nicolson, 1972), wherein proteins and lipids form regions of distinct composition driven by thermodynamic forces. Additionally, liquid ordered (lo) -disordered (ld) phase segregation of lipids was expected to give rise to membrane “rafts” (Simons and Vaz, 2004). These rafts, in turn, were hypothesized to facilitate a number of cellular functions such as the sorting of specific membrane components for the building of signaling complexes, construction of endocytic pits, and transbilayer communication (Simons and Ikonen, 1997).

Because the cell membrane contains a diverse array of lipids with varying acyl chain length/saturation and significant levels of cholesterol, even if the cell membrane is globally mixed and homogeneous at physiological temperatures, it could exhibit small, transient regions with local lo-like character. Indeed, studies using local probes, spin-labeled lipids and electron-spin resonance techniques report deuterium order parameters consistent with the existence of a fraction of membrane lipids exhibiting lo-like conformations (Swamy et al., 2006). However, macroscopic domains are rarely seen in live cells. Studies on the phase behavior of giant plasma membrane-derived vesicles from a number of cell types show that large phase segregated domains form only when these membranes are cooled to temperatures well below physiological temperature (Baumgart et al., 2007) or if some of the membrane components are artificially clustered (Kaiser et al., 2009).

The simple equilibrium picture of phase segregation of membrane composition and order runs into several problems. First, the plasma membrane is an asymmetric multicomponent bilayer; our understanding of phase behavior, local composition heterogeneity, and transbilayer coupling in such systems is preliminary (Polley et al., 2012, 2014). Second, the plasma membrane is attached to an actin cortex, whose role in influencing local membrane composition is poorly understood. Finally, the organization and dynamics of a variety of plasma membrane molecules such as membrane proteins (Gowrishankar et al., 2012; Jaqaman et al., 2011), lipid-anchored proteins (Goswami et al., 2008; Prior et al., 2003; Sharma et al., 2004), and glycolipids (Fujita et al., 2007) into nanometer sized clusters cannot be derived from equilibrium-based mechanisms.

Studies on glycosylphosphatidylinositol (GPI)-anchored proteins (GPI-APs), a large class of plasma membrane proteins located at the exoplasmic (outer) leaflet (Gowrishankar et al., 2012), in particular have demanded a new framework for understanding the local control of molecular organization at the cell surface. Homo-fluorescence resonance energy transfer (FRET)-based fluorescence anisotropy measurements (Sharma et al., 2004; Varma and Mayor, 1998), near-field scanning microscopy (van Zanten et al., 2009), and photoactivation localization microscopy (Sengupta et al., 2011) show that 20%–40% of GPI-APs on the membrane are present as nanoclusters, whereas the rest are monomers. Other studies have shown that monomers are in continuous exchange with relatively immobile nanoclusters (Goswami et al., 2008; Sharma et al., 2004). This organization requires both adequate membrane cholesterol and actin dynamics (Goswami et al., 2008).

GPI-AP clusters are formed by the active engagement of dynamic actin adjacent to the membrane cortex and exhibit unusual properties related to their spatial distribution, small size, temperature-independent fragmentation and formation kinetics, and non-Brownian density fluctuations (Goswami et al., 2008; Gowrishankar et al., 2012). These properties have been explained by a theoretical framework (Chaudhuri et al., 2011; Gowrishankar et al., 2012) based on active contractile mechanics (Marchetti et al., 2013) of dynamic polar filaments. This framework also makes predictions that have been experimentally verified (Gowrishankar et al., 2012). In this mechanism, dynamic actin forms transient contractile regions at the cytoplasmic (inner) leaflet that drive the clustering of the outer leaflet GPI-APs, as well as transmembrane proteins that directly associate with actin filaments.

The actin-driven clustering of GPI-APs requires a coupling of the lipid-tethered protein across the bilayer to the dynamic contractile actin configurations at the inner leaflet. Furthermore, understanding the mechanism of formation of these clusters has a functional significance, both in the sorting of GPI-APs (Mayor and Pagano, 2007; Mayor and Riezman, 2004) and in modulating receptor signaling (Coskun et al., 2011). For example, cholesterol-dependent GPI-AP nanoclustering is necessary for promoting integrin function (van Zanten et al., 2009), which appears to take place in focal adhesions that are surrounded by *lo* domains (Gaus et al., 2006).

Here, we show that this transbilayer coupling requires the long acyl chains of outer leaflet GPI anchors in association with cholesterol and inner leaflet lipids that also carry long acyl chains. We identify phosphatidylserine (PS) as the inner leaflet lipid responsible for this coupling. All-atom molecular dynamic (MD) simulations show that local transbilayer coupling occurs even in membranes that are well above their main transition temperature, provided the long-acyl-chain-containing lipids are immobilized at one leaflet of the bilayer. We show that this immobilization may be mediated by PS binding to actin by constructing a synthetic linker that links PS to actin. Expression of this linker in cells results in coupling of exogenously added lipids with long acyl chains, as well as endogenous GPI-APs, to stable long-lived actin structures located at the inner leaflet.

This supports the idea that dynamic actin filaments at the inner leaflet may have the capacity to immobilize lipids and stabilize local *lo* domains over significant timescales in membranes at physiological temperatures.

RESULTS

Synthetic Fluorescent GPI Analogs with Long Saturated Acyl Chains Mimic GPI-AP Nanoclustering

In mammalian cells, a typical GPI anchor is a complex glycolipid (McConville and Ferguson, 1993), which, in general, possesses long saturated acyl chains either C16:0 or C18:0 (Figure S1A). To test whether the acyl chain length and degree of saturation of the GPI anchor affect nanocluster formation, we generated synthetic GPI analogs (Figure 1A) and studied their nanoclustering ability after their incorporation into the plasma membrane of live cells. The synthesized GPI analogs carry a minimal GPI anchor containing the disaccharide glucosamine-inositol linked to phosphatidic acid (GlcNPI) (instead of the full-

length GPI; Figure S1A). Each analog is conjugated to fluorescent probes to the GPI head group (Figure 1A). The incorporated GPI analogs are retained in the outer leaflet of the plasma membrane as indicated by a complete loss of their fluorescence when subjected to phosphatidylinositol-specific phospholipase-C (PI-PLC) cleavage (Figure S1B). Additional confirmation of their correct membrane incorporation comes from the observation that their diffusion properties also resemble endogenous GPIAPs (Figures S1C and S1D).

Monitoring the fluorescence anisotropy of these synthetic fluorescent GPI analogs—differing only in their acyl chain length as a function of their concentration in the live-cell membrane—provides a measure of the extent of clustering of these analogs (Figure S1E). The fluorescence anisotropy of GPIC16:0/C16:0 is much lower than GPIC8:0/C8:0 (Figures 1B and S2B). It exhibits concentration-independent fluorescence anisotropy over a large concentration range (Figure 1B), similar to endogenous GPI-Aps (Sharma et al., 2004). Consistent with the generation of nanoscale clusters, the photobleaching profiles of the GPIC16:0/C16:0 also mimicked those of fluorescently tagged folic acid analog (PLB-FR-GPI; Figures S1F and S1G). Furthermore, on depleting membrane cholesterol or on disrupting actin activity (blebs devoid of actin were generated by treatment with jasplankinolide [Goswami et al., 2008]), GPIC16:0/C16:0 exhibited an increase in fluorescence anisotropy (Kolmogorov-Smirnov [KS] test $p < 0.001$) (Figures 1D and S2B) similar to PLB-FR-GPI (Figures S2A, S2C, and S2D), suggesting cholesterol and actin-dependent nanoclustering. By contrast, GPIC8:0/C8:0 exhibited a higher fluorescence anisotropy, which did not change upon photobleaching (Figure S1H), cholesterol depletion (Figures 1D and S2B), or actin perturbation, which is consistent with its inability to form nanoclusters in the cell membrane.

Comparable to PLB-FR-GPI, the fluorescence anisotropy of GPIC16:0/C16:0 changes upon photobleaching (Figures S1F and S1G), exhibiting a distinct rise in control cells or on the flat membrane (Figures 1D, S2A–S2D, and S1I). Moreover, the fluorescence anisotropy of both PLB-FR-GPI and the GPIC16:0/C16:0 analog remain unchanged upon photobleaching the bleb fluorescence (Sharma et al., 2004) (Figure S1I), which is consistent with the lack of clusters on the actin-depleted blebs. By contrast, the fluorescence anisotropy of the GPIC8:0/C8:0 on membrane blebs is unaffected by photobleaching (Figures S1H and S1J), confirming its inability to form nanoclusters.

The synthetic GPI analogs allowed us to directly assess the role of (un)saturation in the GPI acyl chains by comparing the clustering abilities of GPIC18:0/C18:0 and GPIC18:1/C18:1. Here, we used fluorescein-tagged GPI analogs, and as observed for its BODIPYTMR-labeled counterpart (Figure 1A), the fluorescence anisotropy of GPIC18:0/C18:0 is concentration independent (Figure 1C) and rises upon cholesterol depletion and in membrane blebs (KS test $p < 0.001$ in both cases) (Figure 1E), which is consistent with formation of nanoclusters. In contrast, the fluorescence anisotropy of GPIC18:1/C18:1 is higher than GPIC18:0/C18:0 (Figure 1C) and does not exhibit a significant change (in comparison to GPIC18:0/C18:0) upon cholesterol depletion or on membrane blebs (Figure 1E), indicating reduced ability to be recruited to nanoclusters. These results suggest that GPI anchor clustering requires long-saturated acyl chain lipids to support actin and cholesterol-based nanoclustering.

GPI-Anchored Protein Nanoclustering Is Abrogated in GPI Anchor Remodeling Mutants

During GPI anchor biosynthesis, cells specifically remodel their unsaturated acyl chains present at the sn-2 position of the immature GPI-anchor to generate long saturated acyl chain lipids (either 16:0 or 18:0) (McConville and Ferguson, 1993). This process of lipid remodeling is mediated by key enzymes, PGAP2 and PGAP3 (Maeda et al., 2007). Cell lines carrying mutations in both PGAP2 and PGAP3 express cell-surface GPI-APs with unremodeled GPI anchors containing unsaturated acyl chains at the sn-2 position of the glycerophospholipid (Maeda et al., 2007). This enabled us to test the requirement of long saturated acyl chains in endogenous GPI-AP nanoclustering. The extent of clustering of the GPI-APs in mutant and wild-type cells was measured by determining the extent of homo-FRET between GPI-APs at the cell surface by monitoring the fluorescence anisotropy of fluorescently tagged FLAER (A488F) (Brodsky et al., 2000). The fluorescence anisotropy in mutant cells is significantly higher (KS test, $p < 0.001$) than that in wild-type cells (Figure 2A) and is similar to the fluorescence anisotropy of A488F-labeled GPI-APs measured in cells treated with a cholesterol sequestering agent, saponin.

Incorporation of GPIC16:0/C16:0 in the plasma membrane of PGAP2/3 mutant cells showed that GPIC16:0/C16:0 clusters to the same extent in both the wild-type and mutant cells (KS test, $p < 0.001$) (Figure 2B), confirming that the lack of nanoclustering in these cell lines is due to the presence of unsaturated lipid tail of GPI-APs and not due to any other artifact that may arise as a result of PGAP2/3 perturbation. These experiments indicate that cholesterol and actin-dependent nanoclustering of endogenous GPI-APs also require long saturated acyl chains in their lipid moiety, which is consistent with results obtained with the synthetic GPI analogs.

Inner Leaflet PS Is Required for GPI-AP Nanoclustering

There are two possibilities by which long-acyl-chain-containing GPI-APs can connect to the actin at the inner leaflet; one involving a transmembrane linker and the other via lipidic interactions across the inner leaflet. To distinguish between these possibilities, we looked into the roles of phosphatidylinositol 4,5-bisphosphate (PI(4,5)P₂) and PS, which are obvious candidates for inner leaflet lipids that could couple outer leaflet GPIAPs with actin. Both of these lipids are also known to interact with several actin-binding proteins (Yin and Janmey, 2003). PS, for example, binds specifically to actin-binding proteins such as spectrin, talin, and various others (Makuch et al., 1997; Muguruma et al., 1995), whereas the Pleckstrin homology (PH) domains present in many proteins interact with PIPs and actin (Yin and Janmey, 2003).

To test the role of these lipids in actin-driven nanoclustering, we expressed protein domains capable of binding PS or PI(4,5)P₂, the most abundant plasma membrane PIPn (Stauffer et al., 1998), to putatively mask the interaction of these lipids with the cytoplasmically disposed actin filaments. We used a fusion construct of GFP with the discoidin-like C2 domain of lactadherin [Lact C2 GFP; Yeung et al., 2008] to mask PS at the inner leaflet and the PH domain of PLCd fused to the NH₂ terminus of GFP protein [PH-GFP; (Stauffer et al., 1998)] for masking PI(4,5)P₂. Cells expressing Lact C2-GFP exhibited higher fluorescence anisotropy of PLB-FR-GPI, which is consistent with a reduction of the extent

of nanoclustering (KS test, $p < 0.001$) (Figures 3A and 3B). This was not due to an alteration in the lipid profile of cells expressing Lact C2-GFP because their lipid composition was unaltered when compared to cells transfected with the GFP alone. Individual lipid classes in transfected cells varied between 93% and 99% of the control values. By contrast, there was no significant effect on the fluorescence anisotropy of PLB-labeled FR-GPI when we expressed PH-GFP (Figures 3A and 3B) nor when PI(4,5)P2 levels were perturbed using an antibiotic such as neomycin or a Phospholipase C activator such as chlorpromazine (Figure S3), indicating the lack of involvement of PI(4,5)P2.

Because GPI-AP nanoclusters depend on actin-based mechanisms, masking PS via the Lact C2 domains could reflect a nonspecific effect of the inaccessibility of PS to cytosolic factors necessary for actin polymerization. To rule out these effects and show that direct association of PS with actin is sufficient for GPI-AP nanoclustering at the outer leaflet, we expressed the Lact C2 domain fused to the actin-filament binding domain of Ezrin (Lact C2-Ez-YFP; Figures 3C and 3D). Similar to the Lact C2 construct, this protein is also recruited to the plasma membrane, in contrast to a cytosolic EGFP control that does not have plasma membrane binding capacity (Figures 3C and 3D). More importantly, only the fusion construct that connects PS to actin restores nanoclustering of GPI-APs (Figures 3C and 3D), emphasizing the role of actin and its ability to link up to PS in facilitating nanocluster formation.

GPI-AP Nanoclustering Requires Long-Acyl-Chain-Containing PS

To explore the nature of the acyl chain on the PS that is involved in coupling with GPI-APs at the outer leaflet, we measured GPI-AP nanoclustering in PS-synthesis-deficient Chinese hamster ovary (CHO) cell lines (PSA3 cells). These cell lines carry a mutation in the PSS1 gene (Nishijima et al., 1986) where the cells are rendered completely dependent on phosphatidylethanolamine (PE) (Figure S4A; Kennedy and Weiss, 1956; Percy et al., 1983). PS levels at the plasma membrane of PSA3 cells grown in absence of ethanolamine (deplete) are drastically reduced compared to cells grown in its presence (replete) (Figures S4B and S4C). To measure the extent of endogenous GPI-AP nanoclustering, we compared the fluorescence anisotropy of the GPI-binding toxin A488F at the surface of PS-depleted and -repleted cells. Nanoclustering of endogenous GPI-AP was disrupted in PS-depleted cells; it is comparable to that obtained in cells depleted of cholesterol (KS test, $p < 0.001$; Figures 4A and 4B). To confirm that the defect in these cells was not due to any perturbation of the endogenous GPI anchor in the PS-deplete condition, we established that, whereas the PS-replete cells were capable of supporting nanoclustering of exogenously added GPIC16:0/C16:0, PS-deplete cells failed to do so (Figures S4D and S4E).

We next replenished the pool of PS in PS-deplete cells by adding various PS species differing in acyl chain length and saturation, and we have confirmed their incorporation at the inner leaflet by the ability to stain with Annexin V only after ionomycin treatment (Figures S4B and S4C). Our results show that only the long alkyl-chain-containing analog is capable of restoring nanoclustering of GPI-APs (Figures 4A, 4B, and 4E: PSC12:0/C12:0*, PSC18:0/C18:0*, PSC18:1/C18:1*), despite the incorporation of all analogs in the membrane at similar levels (Figure S5C). Here, we used synthetic acyl/alkyl PS analogs that

are resistant to phospholipase A2 (PLA2) cleavage (Burke and Dennis, 2009) (Figures 4A, 4B, and 4E; PSC12:0/C12:0*, PSC18:0/C18:0*, and PSC18:1/C18:1*). This experimental strategy was adopted because exogenous addition of any di-acyl PS species restored nanoclustering of endogenous GPI-APs (Figure S4F) in the absence of a PLA2 inhibitor (methyl-arachidonylfluorophosphonate; Figures S4F and S4G). By contrast, in the presence of the PLA2 inhibitor, only the long saturated PSC18:0/18:0 restored GPI-AP nanoclustering, whereas the short and unsaturated lipids, PSC12:0/C12:0 and PSC18:1/C18:1, were incapable of restoring GPI-AP nanoclustering (Figures S4F and S4G). This suggested that PLA2-like enzymes engage in remodeling the acyl chains of exogenously incorporated PS at the inner leaflet. We also found that the exogenous addition of long-acyl-containing PE or PC to the same levels as the PS species (Figure S5B) in PS-deplete conditions does not rescue the nanoclustering of GPI-AP (Figure S4H).

In CHO cells, the most abundant PS species is the asymmetric PSC18:0/C18:1 (Figure S4I), and hence, we determined nanocluster recovery by adding exogenous asymmetric PSC18:0/C18:1 in the presence of PLA2 inhibitor. The restoration of GPI-AP nanoclustering by the addition of the asymmetric lipid was quantitatively equivalent to that of the fully saturated long-chain PSC18:0/C18:0 (Figures 4C and 4D). These results strongly suggest that GPIAPs at the outer leaflet couple across the bilayer with PS with the aid of at least one long saturated chain and adequate cholesterol.

Atomistic MD Simulations Provide a General Mechanism for Transbilayer Coupling

To understand the mechanism by which long-chain GPI and PS lipids couple across the fluid bilayer, we developed atomistic molecular dynamic simulations of membrane bilayers comprising a distinct upper (palmitoyl-oleoyl-phosphatidylcholine [POPC], palmitoyl-sphingomyelin [PSM], and cholesterol [Chol]) and lower leaflet (POPC and Chol) capable of phase segregation into lo and ld phases (Polley et al., 2012, 2014). This approach has allowed an exploration of the effect of lo-ld segregation on either of the two leaflets (Polley et al., 2012, 2014). Here, we examined the regime where both leaflets of the asymmetric bilayer membrane are macroscopically in the homogenous mixed ld phase. We ask under what conditions would trace amounts of GPI on the putative outer (upper) leaflet register with PS in the putative inner (lower) leaflet and what the nature is of this transbilayer coupling. All simulation details, including force fields, tests of approach to thermodynamic equilibrium, and stress profiles at equilibrium are presented in the Extended Experimental Procedures (Figure S6B).

We find that, regardless of chain length/saturation and relative composition, as long as both leaflets of the bilayer are in the ld phase (characterized by low values of the deuterium order parameter S , a measure of the extent of chain ordering), the distribution of GPI and PS is uniform with no transbilayer registry (Figures 5A, S6A, and S6C). However, the situation is entirely different if we cluster and immobilize either PS or GPI (Figures 5A, 5B, and S6A). In this case, we obtain co-segregation and perfect bilayer registry, a situation that represents a constrained equilibrium because of immobilization (Supplemental Information; Figure S6C). Note that the high transbilayer coupling in the ld phase is only obtained at adequate levels of cholesterol in the two leaflets (as shown in Figure 5C). This co-segregation is

accompanied by a steady increase in the local chain stiffness of the membrane components as determined by the local deuterium order parameter S , reflecting local l_0 ordering within the co-segregation region (Figure S6C). A similar dynamics toward co-segregation occurs when the PS starts with a uniform distribution and the GPI is kept immobilized (data not shown). We also study the stability of co-clustering when both GPI and PS are initially clustered at the center with PS held immobile (Figure S6D). From the profile of GPI density and order parameter, we can extract a length scale over which the lipids maintain l_0 -like order (coherence length) as a function of the number of immobilized PS molecules (Figure 5E). The non-linear increase in the coherence length with the number of immobilized PS also reflects the formation of a local l_0 nanodomain.

This transbilayer coupling is surprisingly sensitive to reducing the acyl chain length (or lowering the degree of saturation) of either GPI or PS (Figure S6E), as revealed by the transbilayer correlation coefficient (Figure 5F). This is manifest in the deuterium order parameter profile, which remains small (and close to the l_d value), thus failing to achieve transbilayer coupling that is needed for bilayer registry (Figure S6E). Thus, our atomistic simulations done in the l_d phase of the asymmetric bilayer indicate that it is only in the presence of adequate amounts of cholesterol that the transbilayer coupling of long saturated GPI and PS can be achieved, provided that PS is held immobilized. The lifetime of this co-clustering is therefore set by the lifetime of immobilization of PS. These simulations imply that, in a multicomponent bilayer that is in the mixed l_d phase (not far from the l_0/l_d transition), clustering and immobilization of a few long acyl chain lipids should suffice to effect transbilayer coupling by stabilizing small l_0 -like regions that could spontaneously arise due to proximity to an l_0/l_d transition.

Long Saturated Fatty Acyl Chains of Phospholipids Are Sufficient for Their Nanoclustering

To directly test the predictions of the atomistic MD simulations, we incorporated long acyl-chain-containing synthetic PE analog conjugated to Fluorescein (F-DHPE) in CHO cell membranes and determined its nanoscale organization. Similar to endogenous GPI-APs, fluorescence emission anisotropy of F-DHPE is also concentration independent and increases upon cholesterol depletion and photobleaching (data not shown, but see Figure 6E). Furthermore, incorporation of F-DHPE into PS-deplete cells did not result in nanocluster formation, whereas in PS-replete cells, they form cholesterol-sensitive nanoclusters (Figures 6C and 6D). Consistent with the absence of nanoclusters in PS-deplete cells, the fluorescence anisotropy of F-DHPE also does not increase upon photobleaching. By contrast, there is a rise in anisotropy in PS-replete cells, which is consistent with the presence of PS-dependent nanoclusters of F-DHPE (Figure 6E). This verifies the sufficiency of long saturated acyl chains in facilitating cholesterol-sensitive and PS-mediated nanoclusters of lipids in membranes of live cells.

Immobilization Promotes Transbilayer Coupling Mechanism

To test the role of immobilization in effecting transbilayer coupling of specific lipid components in either leaflet as predicted from our simulations (Figure 5), we determine whether crosslinking outer leaflet GPI-APs into optically resolvable clusters could result in the recruitment of inner leaflet PS molecules to these sites independent of the involvement

of the actin machinery. Alternatively, if we are able to immobilize PS at the inner leaflet, long-acyl-chain-containing species at the outer leaflet should be co-localized to these regions. First, we crosslinked the folate receptor (FR-GPI) at the outer leaflet (Mayor and Maxfield, 1995) and examined the co-distribution of the inner leaflet lipid probes in plasma membrane blebs. In cells expressing Lact C2-GFP, which probes inner-leaflet PS, there is a strong correlation between the intensity distribution of Lact C2-GFP and PLB-FR-GPI, whereas a significantly reduced correlation was observed with PH-GFP, the PIP2 probe (Figures 7A and 7B). Moreover, this correlation reduces upon cholesterol depletion for Lact C2-GFP (KS test, $p < 0.001$) but remains low and unaltered for PH-GFP (Figures 7A and 7B). As a control, we determined whether crosslinking the FR domain linked to transmembrane domain (FR-TM-Ez; Gowrishankar et al., 2012) could recruit Lact C2-GFP. Our results show that there is no significant correlation between crosslinked FR-TM-Ez and Lact C2-GFP (Figures 7A and 7B). These results indicate that PS at the inner leaflet couples strongly with cross-linked GPI-AP patches at the outer leaflet in a cholesterol-sensitive manner. Second, when the actin filament binding Lact C2-Ez-YFP is expressed in CHO cells, it is recruited to the plasma membrane (Figures 3D and 7C), where it is found concentrated on relatively stable actin stress fibers visible at the membrane surface in a TIRF field (Figures 3D and 7C). This provides an experimental handle to visualize actin-immobilized inner leaflet PS. Correspondingly, the fluorescence intensity distribution of an outer leaflet GPIAP and exogenously added DHPE (B-DHPE; Figure 7C) are correlated with regions that show Lact C2-Ez-YFP enrichment. No enrichment of an exogenously added short chain synthetic lipid analog (GPIC8:0/C8:0) is observed in the region of Lact C2-Ez-YFP enrichment (Figure 7C), confirming that this transbilayer coupling requires long acyl chains. The concentrating effect of PS on the outer leaflet lipid is only observed in the presence of an actin-PS connector because this was absent when the F-actin binding domain of Ezrin or the PS-binding domains are expressed on their own (Figure S7), which is consistent with the role of actin and its PS-binding partners in aiding the formation of nanoclusters. Taken together, the experiments point toward a general mechanism underlying transbilayer coupling where either of the outer or inner leaflet molecules need to be immobilized.

DISCUSSION

Our experimental and simulation results provide evidence that nanoclustering of outer leaflet GPI-APs and indeed any outer leaflet lipid by dynamic cortical actin is effected by the interdigitation and transbilayer coupling of lipids having long, saturated acyl chains, both in the outer and inner leaflets of the PM. This is contingent on properties of the lipid acyl chains, adequate cholesterol levels in the bilayer, and immobilization of the inner leaflet lipid. In contrast to transmembrane-anchored actin binding proteins, which straddle the bilayer, these three features allow for a flexibility and regulation of transbilayer communication of lipids.

The requirement for long acyl or alkyl chains to couple across the bilayer provides a purely lipidic coupling mechanism, obviating the need for any transmembrane protein coupling mechanism. This could also serve as a way to couple many outer leaflet membrane lipids such as Gangliosides and other sphingolipids (Wolf et al., 1998). The results from

simulations show that cholesterol can stabilize local lo-like order over a length scale that is larger than the size of the immobilized cluster, suggesting that it might also engage in recruiting more components via a positive feedback mechanism leading to a composition gradient of components that favor lo domains.

The immobilization of the inner leaflet lipid relates to the mechanism needed for nanoclustering. In the atomistic MD simulations, carried out for a timescale of 200 ns (and reconfirmed by longer 1 ms runs; Supplemental Information), transbilayer coupling requires immobilization of PS lipid; the removal of anchoring leads to a rapid loss of clustering of the lipids at both leaflets. We had previously shown that GPI-AP nanoclusters are “immobile” for a period of 0.1–1 s (Goswami et al., 2008). This could reflect the time of engagement of dynamic cortical actin filaments at the inner surface of the cell membrane (Gowrishankar et al., 2012). Additionally, immobilization of more than one lipid molecule is necessary to create the transbilayer connection; more molecules need to be immobilized, depending on how far the membrane composition is maintained away from the equilibrium lo-ld phase transition in order to couple across the bilayer.

Synthetic lipids with long acyl chains couple across the bilayer, forming dynamic actin-based nanoclusters; this mechanism is therefore capable of clustering any endogenous outer leaflet lipid species with long acyl chains if the inner leaflet lipid is sufficiently immobilized. Indeed, coupling of PS to a stable actin template such as a stress fiber via a synthetic PS-actin bridge (Lact C2- Ez-YFP) also served to recruit endogenous GPI-APs and exogenously added long-chain lipids (F-DHPE), but not short-chain lipids. Given that the nanoclusters formed by the contractile actin-based clustering machinery exhibit nanoscale clusters that appear to be co-segregated (Goswami et al., 2008; vanZanten et al., 2009), this observation suggests that domains that are enriched in nanoclusters created by the transbilayer coupling mechanism will have lo-like character. Consistent with this, recent evidence from our group indicates that regions enriched in GPI-APs nanoclusters exhibit “lo”-like properties (Suvrajit Saha, A.A.A., and S.M., unpublished data). Together, these principles provide a very general mechanism whereby immobilizing an appropriate inner or outer leaflet lipid with long saturated acyl chains can help stabilize local lo domains even in a predominantly homogenous, mixed ld membrane.

We show that the co-segregation of GPI and PS is achieved when GPI is clustered and immobilized in the outer leaflet while allowing PS to equilibrate and vice versa. This has implications for the construction of cell-surface signaling platforms or sorting platforms at the inner leaflet by crosslinking long saturated GPI anchored proteins (Stefanová et al., 1991; Suzuki et al., 2007; Wolf et al., 1998). Here, the clustering of GPI-APs at the outer leaflet appears to build complexes at the inner leaflet to effect specific signaling reactions. Additionally, local lipid organization plays a crucial role in the nanoclustering of cell-surface Ras molecules, thereby regulating signaling mechanisms locally (Ariotti et al., 2014). Inefficient coupling across the membrane can impair several cell-signaling events and can lead to major immune response and neurodegenerative disorders. For instance, deletion of PGAP3 results in enhanced T cell receptor signaling, as evaluated in PGAP3 knockout mice (Murakami et al., 2012), and a mutation in PGAP3 leads to a subtype of

hyperphosphatasia with intellectual disorders commonly referred to as Mabry syndrome (Howard et al., 2014).

Finally, PS must in turn be connected to endogenous actin binding proteins. The capacity of the synthetic PS and actin binding fusion protein (LactC2-Ez-YFP) to reconstruct actin based nanoclustering provides strong support for this idea. Several examples of such proteins exist such as talin (Muguruma et al., 1995), spectrin (An et al., 2004), caldesmon (Makuch et al., 1997), myosin 1A (Mazerik and Tyska, 2012), and vinculin (Ito et al., 1983), and to completely elucidate the mechanism of transbilayer coupling to actin, the identity of this coupling agent(s) needs to be determined.

In conclusion, we show that lipidic interactions mediated by long-chain interdigitation in the presence of cholesterol stabilize a transbilayer connection between outer and inner leaflet lipids when either of the lipid species is immobilized. The deployment of this mechanism in the mixed phase of the bilayer by active clusters of actin filaments, which can engage PS at the inner leaflet, provide a general mechanism to stabilize these lo domains locally. The formation of the contractile actin clusters would then determine when and where these domains may be stabilized, bringing the generation of membrane domains in live cells under control of the actomyosin signaling network.

EXPERIMENTAL PROCEDURES

Detailed experimental conditions are provided in the Extended Experimental Procedures in the Supplemental Information.

Plasmids, Cell Lines, Antibodies, and Other Reagents

CHO cell lines stably expressing folate receptor (IA2.2; Mayor and Maxfield, 1995) or carrying mutations in PGAP2 and 3 (PGAP2/3; Maeda et al., 2007), PSA3 (PSA3; Nishijima et al., 1986), C term Ez GFP, and PH-GFP were obtained from several sources as indicated in the Supplemental Information. IA2.2 cells, PSA3 cells, PGAP2/3 double-mutant cells, and FR-TM-Ez cells were maintained in Ham's F12 medium with an appropriate concentration of antibiotics as mentioned in the Supplemental Information.

GPI and PS Analogs

The synthesis of fluorescently tagged GPI analogs and PLA2-resistant PS analogs is described in detail in the Extended Experimental Procedures.

GPI Analog and Lipid Incorporation

Synthetic GPI analogs were incorporated into cell membranes by the g-CD method (Koivusalo et al., 2007), whereas PS analogs were incorporated by Lipofectamine method as described (Saha et al., 2015).

Diffusion Measurements

Fluorescence correlation spectroscopy (FCS) and fluorescence recovery after photobleaching (FRAP) measurements to determine proper incorporation were performed as described previously (Gowrishankar et al., 2012).

PI-PLC Treatment

PI-PLC was purified in the laboratory from *Bacillus thuringiensis* as reported (Kobayashi et al., 1996). Cells cooled on ice were incubated with PI-PLC (0.5 U/ml) for 1 hr and then washed with M1 and imaged live.

Anisotropy Measurements

Steady-state homo-FRET-based anisotropy measurements were carried out on a NikonTE2000 epifluorescence microscope equipped with an Andor TuCam dual camera imaging arrangement in the TIRF, spinning-disc confocal, or wide-field mode (Ghosh et al., 2012).

Treatments to Perturb Inner Leaflet Lipids, PIP2 and PS

To perturb PIP2, CHO cells were treated with either neomycin (10 mM) or chlorpromazine (10 mM) for 15 min at 37_C as described (Arbuzova et al., 2000; Raucher and Sheetz, 2001). For perturbation of PS levels, PSA3 cells were grown under replete (cells grown in the presence of 10 mM ethanolamine) or deplete (cells grown in dialysed serum for 48 hr) conditions. PS levels were measured by assessing the extent of Annexin V binding as detailed in the Supplemental Information.

Lipid Analysis and Mass Spectrometry Experiments

Lipids analysis was carried out on FACS sorted cells expressing specific transgenes (Lact C2-GFP or GFP) or on membrane blebs prepared from cells as detailed previously (Pick et al., 2005). Lipid extraction was done by Bligh and Dyer method (Bligh and Dyer, 1959), and mass spectrometry measurements were carried out on an LTQ Orbitrap XL hybrid mass spectrometer (Thermo Fisher Scientific).

Atomistic MD Simulations

We perform an all-atom MD simulation of the asymmetric, multi-component bilayer with POPC, cholesterol (Chol), and PSM in the upper leaflet and POPC and cholesterol in the lower leaflet at 23_C. GPI-AP and PS are inserted in the upper and lower leaflets, respectively. The relative composition of the bilayer is varied, and the detailed experimental procedures and simulation conditions are provided in the Supplemental Information. The membrane bilayers were equilibrated and deemed to be mechanically stable prior to determining the distribution of various constituents. Immobilization of a molecular species is achieved by setting a high value to its mass without affecting other features of the simulation (Supplemental Information).

Supplementary Material

Refer to Web version on PubMed Central for supplementary material.

ACKNOWLEDGMENTS

We thank Suvrajit Saha for help with FCS measurements and MEM analysis; Balaji for Matlab codes to analyze the anisotropy data; Kabir Husain for help with the correlation analysis; Joseph Jose Thottacherry and Darius Koester for FRAP measurement and analysis; Taroh Kinoshita, Tomohiko Taguchi, Tobias Meyer, and Antonio S. Sechi for their generous gifts of various reagents(as indicated in the Supplemental Information); Max Planck-NCBS lipid centre; Dominik Schwudke and Sudarkodi Sukumar for mass spectrometry; and H. Krishnamurthy and Manoj Mathew at the Central Imaging and Flow Facility (NCBS). R.R. acknowledges Vytas A. Bankaitis for suggestions with lipid incorporation methods. We thank Tampere University of Technology for help with the longer run simulations and all SM lab members for their critical comments on the manuscript. S.M. acknowledges JC Bose Fellowship from DST (Government of India) and a grant from HFSP RGP0027/2012. A.A.A. acknowledges pre-doctoral fellowship from CSIR. M.R. acknowledges a grant from Simons Foundation. Z.G. acknowledges NSF CHE-1053848 and NIH GM090270 for providing financial support.

REFERENCES

- An X, Guo X, Wu Y, Mohandas N. Phosphatidylserine binding sites in red cell spectrin. *Blood Cells Mol. Dis.* 2004; 32:430–432. [PubMed: 15121103]
- Arbuzova A, Martushova K, Hangyás-Mihályiné G, Morris AJ, Ozaki S, Prestwich GD, McLaughlin S. Fluorescently labeled neomycin as a probe of phosphatidylinositol-4, 5-bisphosphate in membranes. *Biochim. Biophys. Acta.* 2000; 1464:35–48. [PubMed: 10704918]
- Ariotti N, Fernández-Rojo MA, Zhou Y, Hill MM, Rodkey TL, Inder KL, Tanner LB, Wenk MR, Hancock JF, Parton RG. Caveolae regulate the nanoscale organization of the plasma membrane to remotely control Ras signaling. *J. Cell Biol.* 2014; 204:777–792. [PubMed: 24567358]
- Baumgart T, Hammond AT, Sengupta P, Hess ST, Holowka DA, Baird BA, Webb WW. Large-scale fluid/fluid phase separation of proteins and lipids in giant plasma membrane vesicles. *Proc. Natl. Acad. Sci. USA.* 2007; 104:3165–3170. [PubMed: 17360623]
- Bligh EG, Dyer WJ. A rapid method of total lipid extraction and purification. *Can. J. Biochem. Physiol.* 1959; 37:911–917. [PubMed: 13671378]
- Brodsky RA, Mukhina GL, Li S, Nelson KL, Chiurazzi PL, Buckley JT, Borowitz MJ. Improved detection and characterization of paroxysmal nocturnal hemoglobinuria using fluorescent aerolysin. *Am. J. Clin. Pathol.* 2000; 114:459–466. [PubMed: 10989647]
- Burke JE, Dennis EA. Phospholipase A2 structure/function, mechanism, and signaling. *J. Lipid Res.* 2009; 50:S237–S242. [PubMed: 19011112]
- Chaudhuri A, Bhattacharya B, Gowrishankar K, Mayor S, Rao M. Spatiotemporal regulation of chemical reactions by active cytoskeletal remodeling. *Proc. Natl. Acad. Sci. USA.* 2011; 108:14825–14830. [PubMed: 21873247]
- Coskun U, Grzybek M, Drechsel D, Simons K. Regulation of human EGF receptor by lipids. *Proc. Natl. Acad. Sci. USA.* 2011; 108:9044–9048. [PubMed: 21571640]
- Fujita A, Cheng J, Hirakawa M, Furukawa K, Kusunoki S, Fujimoto T. Gangliosides GM1 and GM3 in the living cell membrane form clusters susceptible to cholesterol depletion and chilling. *Mol. Biol. Cell.* 2007; 18:2112–2122. [PubMed: 17392511]
- Gaus K, Le Lay S, Balasubramanian N, Schwartz MA. Integrin-mediated adhesion regulates membrane order. *J. Cell Biol.* 2006; 174:725–734. [PubMed: 16943184]
- Ghosh S, Saha S, Goswami D, Bilgrami S, Mayor S. Dynamic imaging of homo-FRET in live cells by fluorescence anisotropy microscopy. *Methods Enzymol.* 2012; 505:291–327. [PubMed: 22289460]
- Goswami D, Gowrishankar K, Bilgrami S, Ghosh S, Raghupathy R, Chadda R, Vishwakarma R, Rao M, Mayor S. Nanoclusters of GPI-anchored proteins are formed by cortical actin-driven activity. *Cell.* 2008; 135:1085–1097. [PubMed: 19070578]

- Gowrishankar K, Ghosh S, Saha S, C R, Mayor S, Rao M. Active remodeling of cortical actin regulates spatiotemporal organization of cell surface molecules. *Cell*. 2012; 149:1353–1367. [PubMed: 22682254]
- Howard MF, Murakami Y, Pagnamenta AT, Daumer-Haas C, Fischer B, Hecht J, Keays DA, Knight SJL, Kölsch U, Krüger U, et al. Mutations in PGAP3 impair GPI-anchor maturation, causing a subtype of hyperphosphatasia with mental retardation. *Am. J. Hum. Genet.* 2014; 94:278–287. [PubMed: 24439110]
- Ito S, Werth DK, Richert ND, Pastan I. Vinculin phosphorylation by the src kinase. Interaction of vinculin with phospholipid vesicles. *J. Biol. Chem.* 1983; 258:14626–14631. [PubMed: 6417142]
- Jaqaman K, Kuwata H, Touret N, Collins R, Trimble WS, Danuser G, Grinstein S. Cytoskeletal control of CD36 diffusion promotes its receptor and signaling function. *Cell*. 2011; 146:593–606. [PubMed: 21854984]
- Kaiser HJ, Lingwood D, Levental I, Sampaio JL, Kalvodova L, Rajendran L, Simons K. Order of lipid phases in model and plasma membranes. *Proc. Natl. Acad. Sci. USA.* 2009; 106:16645–16650. [PubMed: 19805351]
- Kennedy EP, Weiss SB. The function of cytidine coenzymes in the biosynthesis of phospholipides. *J. Biol. Chem.* 1956; 222:193–214. [PubMed: 13366993]
- Kobayashi T, Tamura H, Taguchi R, Udaka S, Ikezawa H. High-level expression of *Bacillus thuringiensis* phosphatidylinositol-specific phospholipase C by the *Bacillus brevis* host-vector system. *Jpn. J. Med. Sci. Biol.* 1996; 49:103–112. [PubMed: 8950642]
- Koivusalo M, Jansen M, Somerharju P, Ikonen E. Endocytic trafficking of sphingomyelin depends on its acyl chain length. *Mol. Biol. Cell.* 2007; 18:5113–5123. [PubMed: 17942604]
- Kumari S, Mayor S. ARF1 is directly involved in dynamin-independent endocytosis. *Nat. Cell Biol.* 2008; 10:30–41. [PubMed: 18084285]
- Maeda Y, Tashima Y, Houjou T, Fujita M, Yoko-o T, Jigami Y, Taguchi R, Kinoshita T. Fatty acid remodeling of GPI-anchored proteins is required for their raft association. *Mol. Biol. Cell.* 2007; 18:1497–1506. [PubMed: 17314402]
- Makuch R, Zasada A, Mabuchi K, Krauze K, Wang CLAL, Dabrowska R. Phosphatidylserine liposomes can be tethered by caldesmon to actin filaments. *Biophys. J.* 1997; 73:1607–1616. [PubMed: 9284327]
- Marchetti MC, Joanny JF, Ramaswamy S, Liverpool TB, Prost J, Rao M, Simha RA. Hydrodynamics of soft active matter. *Rev. Mod. Phys.* 2013; 85:1143–1189.
- Mayor S, Maxfield FR. Insolubility and redistribution of GPI anchored proteins at the cell surface after detergent treatment. *Mol. Biol. Cell.* 1995; 6:929–944. [PubMed: 7579703]
- Mayor S, Pagano RE. Pathways of clathrin-independent endocytosis. *Nat. Rev. Mol. Cell Biol.* 2007; 8:603–612. [PubMed: 17609668]
- Mayor S, Riezman H. Sorting GPI-anchored proteins. *Nat. Rev. Mol. Cell Biol.* 2004; 5:110–120. [PubMed: 15040444]
- Mazerik JN, Tyska MJ. Myosin-1A targets to microvilli using multiple membrane binding motifs in the tail homology 1 (TH1) domain. *J. Biol. Chem.* 2012; 287:13104–13115. [PubMed: 22367206]
- McConville MJ, Ferguson MA. The structure, biosynthesis and function of glycosylated phosphatidylinositols in the parasitic protozoa and higher eukaryotes. *Biochem. J.* 1993; 294:305–324. [PubMed: 8373346]
- Muguruma M, Nishimuta S, Tomisaka Y, Ito T, Matsumura S. Organization of the functional domains in membrane cytoskeletal protein talin. *J. Biochem.* 1995; 117:1036–1042. [PubMed: 8586616]
- Murakami H, Wang Y, Hasuwa H, Maeda Y, Kinoshita T, Murakami Y. Enhanced response of T lymphocytes from *Pgap3* knockout mouse: Insight into roles of fatty acid remodeling of GPI anchored proteins. *Biochem. Biophys. Res. Commun.* 2012; 417:1235–1241. [PubMed: 22227195]
- Nishijima M, Kuge O, Akamatsu Y. Phosphatidylserine biosynthesis in cultured Chinese hamster ovary cells. I. Inhibition of de novo phosphatidylserine biosynthesis by exogenous phosphatidylserine and its efficient incorporation. *J. Biol. Chem.* 1986; 261:5784–5789. [PubMed: 3700372]

- Percy AK, Moore JF, Carson MA, Waechter CJ. Characterization of brain phosphatidylserine decarboxylase: localization in the mitochondrial inner membrane. *Arch. Biochem. Biophys.* 1983; 223:484–494. [PubMed: 6859873]
- Pick H, Schmid EL, Tairi A, Ilegems E, Hovius R, Vogel H. Investigating cellular signaling reactions in single attoliter vesicles. *J. Am. Chem. Soc.* 2005; 8:2908–2912. [PubMed: 15740126]
- Polley A, Vemparala S, Rao M. Atomistic simulations of a multicomponent asymmetric lipid bilayer. *J. Phys. Chem. B.* 2012; 116:13403–13410. [PubMed: 23088327]
- Polley A, Mayor S, Rao M. Bilayer registry in a multicomponent asymmetric membrane: dependence on lipid composition and chain length. *J. Chem. Phys.* 2014; 141:064903. [PubMed: 25134595]
- Prior IA, Muncke C, Parton RG, Hancock JF. Direct visualization of Ras proteins in spatially distinct cell surface microdomains. *J. Cell Biol.* 2003; 160:165–170. [PubMed: 12527752]
- Raucher D, Sheetz MP. Phospholipase C activation by anesthetics decreases membrane-cytoskeleton adhesion. *J. Cell Sci.* 2001; 114:3759–3766. [PubMed: 11707527]
- Saha S, Raghupathy R, Mayor S. Homo-FRET imaging highlights the nanoscale organization of cell surface molecules. *Methods Mol. Biol.* 2015; 1251:151–173. [PubMed: 25391799]
- Sengupta P, Jovanovic-Taliman T, Skoko D, Renz M, Veatch SL, Lippincott-Schwartz J. Probing protein heterogeneity in the plasma membrane using PALM and pair correlation analysis. *Nat. Methods.* 2011; 8:969–975. [PubMed: 21926998]
- Sharma P, Varma R, Sarasij RC, Ira, Gousset K, Krishnamoorthy G, Rao M, Mayor S. Nanoscale organization of multiple GPIanchored proteins in living cell membranes. *Cell.* 2004; 116:577–589. [PubMed: 14980224]
- Simons K, Ikonen E. Functional rafts in cell membranes. *Nature.* 1997; 387:569–572. [PubMed: 9177342]
- Simons K, Vaz WLC. Model systems, lipid rafts, and cell membranes. *Annu. Rev. Biophys. Biomol. Struct.* 2004; 33:269–295. [PubMed: 15139814]
- Singer SJ, Nicolson GL. The fluid mosaic model of the structure of cell membranes. *Science.* 1972; 175:720–731. [PubMed: 4333397]
- Stauffer TP, Ahn S, Meyer T. Receptor-induced transient reduction in plasmamembrane PtdIns(4,5)P2 concentration monitored in living cells. *Curr. Biol.* 1998; 8:343–346. [PubMed: 9512420]
- Stefanová I, Horejsí V, Ansotegui IJ, Knapp W, Stockinger H. GPI-anchored cell-surface molecules complexed to protein tyrosine kinases. *Science.* 1991; 254:1016–1019. [PubMed: 1719635]
- Suzuki KGN, Fujiwara TK, Sanematsu F, Iino R, Edidin M, Kusumi A. GPI-anchored receptor clusters transiently recruit Lyn and G alpha for temporary cluster immobilization and Lyn activation: single-molecule tracking study 1. *J. Cell Biol.* 2007; 177:717–730. [PubMed: 17517964]
- Swamy MJ, Ciani L, Ge M, Smith AK, Holowka D, Baird B, Freed JH. Coexisting domains in the plasma membranes of live cells characterized by spin-label ESR spectroscopy. *Biophys. J.* 2006; 90:4452–4465. [PubMed: 16565045]
- van Zanten TS, Cambi A, Koopman M, Joosten B, Figdor CG, Garcia-Parajo MF. Hotspots of GPI-anchored proteins and integrin nanoclusters function as nucleation sites for cell adhesion. *Proc. Natl. Acad. Sci. USA.* 2009; 106:18557–18562. [PubMed: 19850864]
- Varma R, Mayor S. GPI-anchored proteins are organized in submicron domains at the cell surface. *Nature.* 1998; 394:798–801. [PubMed: 9723621]
- Wolf AA, Jobling MG, Wimer-Mackin S, Ferguson-Maltzman M, Madara JL, Holmes RK, Lencer WI, Ruston S, Madara JL, Hirst T. Ganglioside structure dictates signal transduction by cholera toxin and association with caveolae-like membrane domains in polarized epithelia. *J. Cell Biol.* 1998; 141:917–927. [PubMed: 9585411]
- Yeung T, Gilbert GE, Shi J, Silvius J, Kapus A, Grinstein S. Membrane phosphatidylserine regulates surface charge and protein localization. *Science.* 2008; 319:210–213. [PubMed: 18187657]
- Yin HL, Janmey PA. Phosphoinositide regulation of the actin cytoskeleton. *Annu. Rev. Physiol.* 2003; 65:761–789. [PubMed: 12471164]

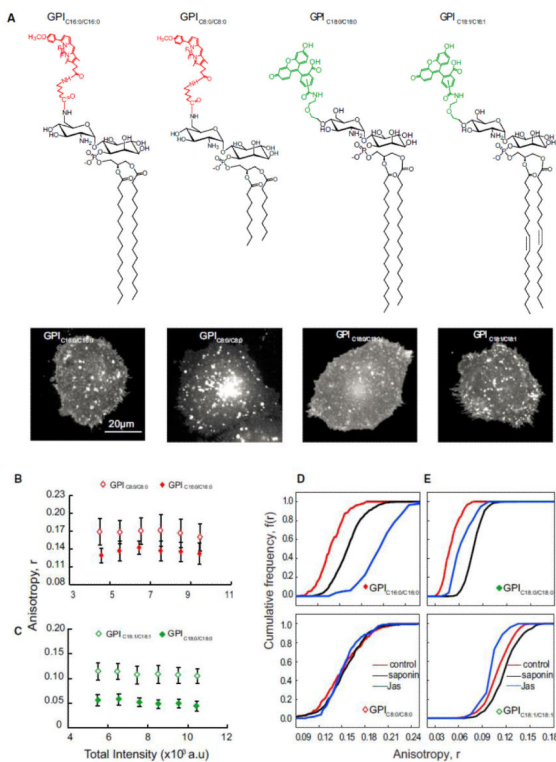


Figure 1.

Long-Saturated-Acyl-Chain-Containing GPIs Support Nanoclustering (A–E) Chemical structures of synthetic minimal GPI analogs (A) outline the variation in the di-acyl glycerolipid chain length (C16:0 and C8:0) and saturation (C18:0 and C18:1) used in this study. GlcNPI carry fluorescent labels BODIPYTMR (left) or fluorescein (right). Representative gray scale images of CHO (IA2.2F) cells with exogenously incorporated GPI analogs as indicated are shown below each analog. Fluorescence anisotropy of GPIC16:0/C16:0 (red closed diamonds) or GPIC18:0/C18:0 (green closed diamonds) in comparison to GPIC8:0/C8:0 (red open diamonds) or GPIC18:1/C18:1 (green open diamonds) determined from images as above were plotted against a wide range of intensity of fluorescent GPI analogs available at the membrane of live cells. Scale bar, 20 mm (B, C). Cumulative frequency distributions (CFD) derived from data derived from identical intensity ranges of GPIC16:0/C16:0 and GPIC8:0/C8:0 (D) or GPIC18:0/C18:0 and GPIC18:1/C18:1 (E) incorporated into cells show the effect of cholesterol depletion by saponin treatment (sap; black line) or on blebs prepared by treatment with jasplakinolide (jas, blue lines) with respect to untreated cells (control, red lines). Each data point in the graphs represents average anisotropy with SD for the corresponding intensity bin obtained from a 10310 pixel region (20–50 regions per cell) from at least 40 cells from 2 independent experiments. Error bars represent SD. See also Figures S1 and S2.

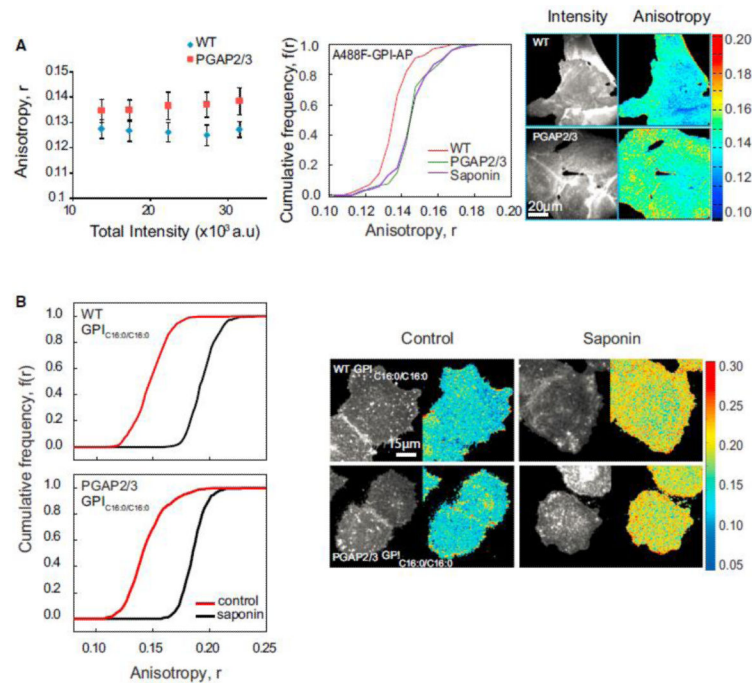


Figure 2.

GPI-AP Nanoclustering Is Reduced in GPI Anchor Lipid Remodeling Mutants (A and B) Fluorescence anisotropy of fluorescently tagged FLAER_ (Alexa-488-FLAER, A488F) in wild-type and PGAP2/3 double-mutant CHO cells (blue diamonds and red squares, respectively) plotted against fluorescence intensity shows an increase in anisotropy in mutant cells (A), corresponding to a loss of homo-FRET between A488F-labeled GPI-APs. Intensity and anisotropy were determined from images collected from cells as shown on the right. CFD plots and images (A) for wild-type (red line), PGAP2/3 double-mutant (green line) and saponin treated (violet line) cells and (B) for GPIC16:0/C16:0 in control (red line), and cholesterol-depleted (black line) conditions in WT and PGAP2/3 mutant cells. CFD plots show that A488F-labeled GPI-APs in mutant cells exhibit an increase in anisotropy compared to wild-type cells and exogenously incorporated GPIC16:0/C16:0 exhibit significantly depolarized fluorescence anisotropy (control) in both wild-type (top) and mutant cells (bottom) that is sensitive to cholesterol depletion by saponin (black line). Each data point in the graphs and CFDs represents average anisotropy values derived from nearly 40 cells from 3 independent experiments. Error bars represent SD.

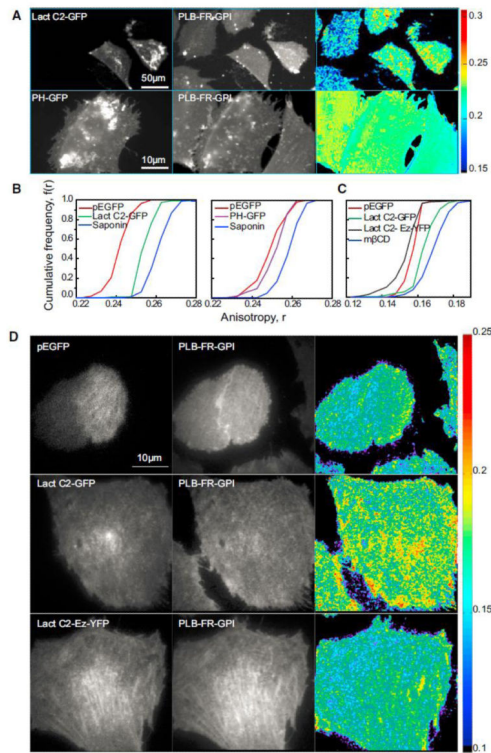


Figure 3.

Masking of PS Binding Sites Alters GPI-AP Nanocluster Organization (A–D) Cropped fluorescence intensity and anisotropy images of FR-GPI-expressing CHO cells (A and D) transfected with EGFP, EGFP tagged to C2 domain of lactadherin (Lact C2 GFP), PH domain of PLCd (PH GFP), or a fusion construct of Lact C2 and actin binding domain (Lact C2-Ez-YFP) and corresponding CFD plots (B and C) were obtained from wide-field (A and B) and TIRF (C and D) microscopes, respectively. The fluorescence anisotropy of PLB bound to FR-GPI in cells expressing EGFP (red line) is comparable to that obtained in PH-GFP (violet line, middle) or Lact C2-Ez-YFP (black line, right) but is increased in cells expressing Lact C2-GFP (green line, left or right). This is in turn comparable to cells treated with saponin or mbCD (blue line). See also Figure S3.

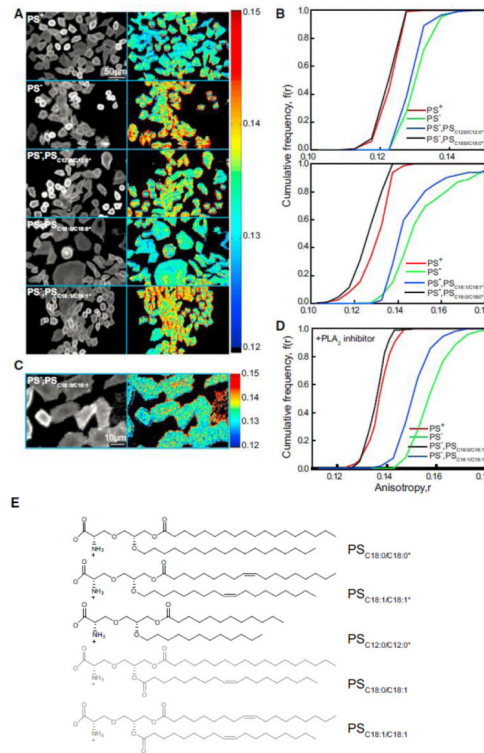
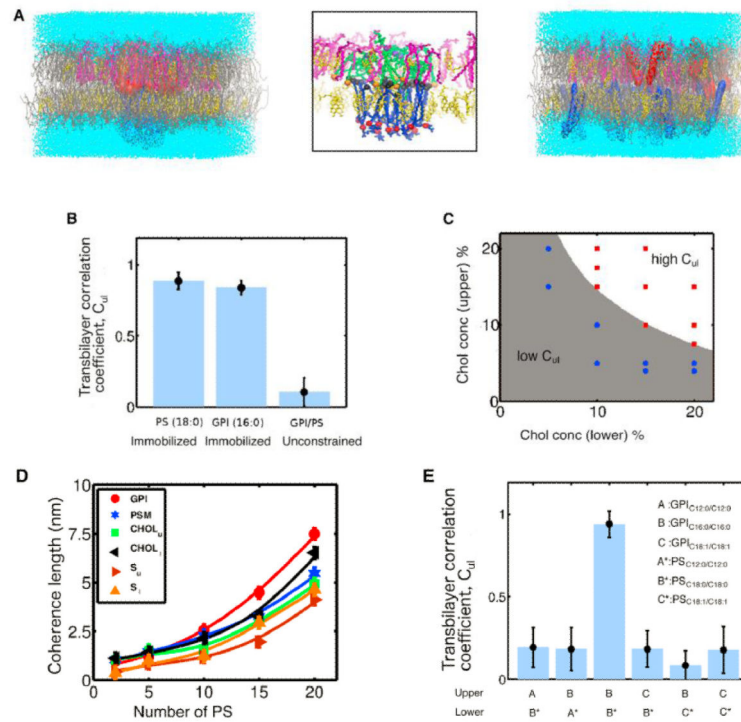


Figure 4.

Nanoclustering of GPI-AP at the Cell Surface Requires Long-Acyl-Chain-Containing PS (A–D) Cropped fluorescence intensity and anisotropy images (A and C) and cumulative frequency distributions (B and D) of A488F-labeled PSA3 mutant CHO cells grown with (PS replete [PS⁺; red line] or without [PS deplete (PS⁻); green line]) ethanolamine and supplemented with PLA₂-insensitive PS analogs of indicated acyl chain lengths and saturation (A and B; blue or black line) or supplemented with PLA₂ inhibitor and PLA₂-sensitive PS analogs of indicated acyl chain saturation (C and D; blue and black lines). (E) Chemical structure depicts the PLA₂-insensitive (black) and -sensitive (gray) PS analogs used in (A)–(D) above, respectively.

See also Figures S4 and S5.

**Figure 5.**

Atomistic MD Simulations Capture Transbilayer Interdigitation of Long Acyl Chain Lipids (A) Equilibrium configurations of an asymmetric bilayer composed of POPC (gray), PSM (magenta), Chol (yellow), GPI (red or green), and PS (blue) embedded in water (cyan) from MDsimulations in the *l_d* phase. Upper leaflet comprises 4% PSM, 4% Chol, 10 long saturated GPIC16:0/C16:0, and the rest POPC, whereas lower leaflet has 35% Chol, 25 long saturated PS C18:0/C18:0, and the rest POPC when PS is not constrained (right, Figure S6A) or when PS molecules are immobilized (left and middle) which, when zoomed (middle), shows bilayer registry and interdigitation of GPI and PS. Local region surrounding interdigitating PS and GPI consists of enhanced levels of PSM and Chol, resembling local *l_o*-like nanodomain. (B) Extent of bilayer registry between GPI and PS measured by the transbilayer correlation coefficient C_{ul} (Experimental Procedures), which takes values 1 (0) when bilayer registry is strong (weak). Data shown are for the same bilayer composition as in (A) above. Transbilayer coupling C_{ul} is significant only when either PS or GPI are held in a cluster and immobilized. There is no transbilayer coupling and hence no registry when the GPI and PS are unconstrained. (C) Levels of cholesterol in upper/lower leaflets that are needed to obtain high transbilayer coupling C_{ul} in the *l_d* phase (white [high C_{ul}] or gray [low C_{ul}]). The cholesterol concentrations in the two leaflets are varied as shown (dots), the upper leaflet has 10 GPI, and the lower leaflet has 15 PS, with POPC contributing to the rest. PSM concentration at the upper leaflet is same as cholesterol. Red (blue) dots designate high C_{ul} y1 (low, C_{ul} 0). (D) Coherence length of membrane component density and deuterium order parameter in the two leaflets at late times when PS is held immobilized, computed from the exponential decay of their profiles. Coherence length increases non-linearly with the number of immobilized PS. Composition in upper leaflet is 92% POPC, 4%

PSM, 4% Chol, and 10 GPI and in lower leaflet is 65% POPC, 35% Chol with number of PS varying from 2 to 20. (E) Transbilayer coupling, C_{ul} between GPI and PS is sensitive to lipid chain length and degree of saturation of acyl chains. Composition of upper leaflet is 33.3% PSM, 33.3% Chol, 10 GPI, and the rest POPC; the composition of the lower leaflet is 10% PS, 10% Chol, and the rest POPC. Chain length and degree of saturation of PS and GPI are varied as indicated. Strong transbilayer coupling and bilayer registry are obtained only when both PS and GPI have long saturated acyl chains. Error bars represent SD. See also Figure S6.

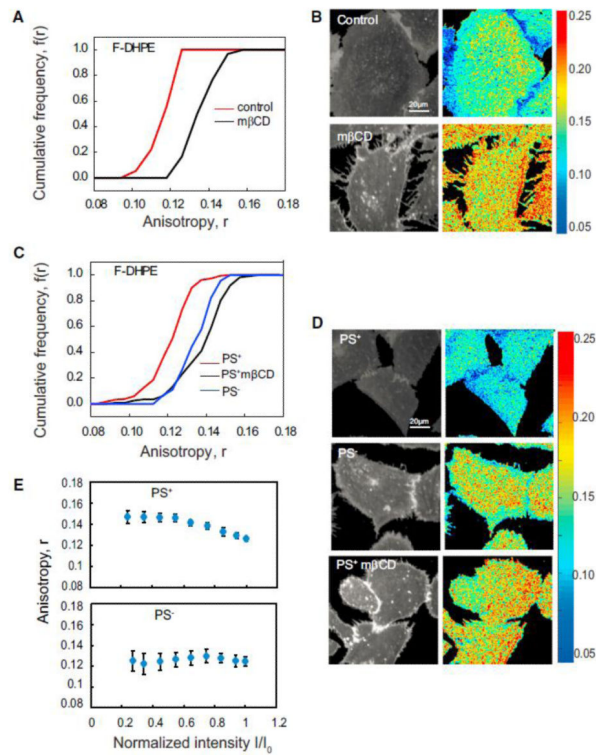


Figure 6.

Lipids with Long Saturated Acyl Chains Are Sufficient to Drive Nanocluster Formation (A–D) Cumulative frequency distribution (A and C) and fluorescence intensity and anisotropy images (B and D) of F-DHPE incorporated in control (IA2.2F) cells (A and B) and PSS1-deficient (PSA3) CHO cells (C and D) show that the fluorescence anisotropy of F-DHPE in control cells and PS replete (control, PS+; red line) is depolarized compared to that measured in cholesterol depleted (black line) or PS-deficient (PS₋) cells (blue line). Note that fluorescence anisotropy of FDHPE in PS deplete (PS₋) cells (blue line) is similar to that measured in saponin-treated cells (black line). Each data point in the graphs represents average anisotropy with SD for the corresponding intensity bin obtained from a 10310 pixel region (20–50 regions per cell) from at least 40 cells derived from two independent experiments. (E) Photobleaching profiles of F-DHPE incorporated into PS replete (PS₊) cells and PS deplete (PS₋) cells. PS replete (PS₊) cells and PS deplete (PS₋) cells were incorporated with exogenously added F-DHPE (E) photobleached and the fluorescence emission anisotropy recorded during the photobleaching process. Note that the profiles of change in fluorescence anisotropy upon change in fluorescence intensity in case of PS replete (PS₊) cells are characteristic of nanoclustered fluorophores (Sharma et al., 2004), whereas PS deplete (PS₋) cells exhibit no change, indicating the lack of homo-FRET. The starting intensity for all the samples collected here is similar and normalized to that used in the first frame.

Error bars represent SD. See also Figure S4.

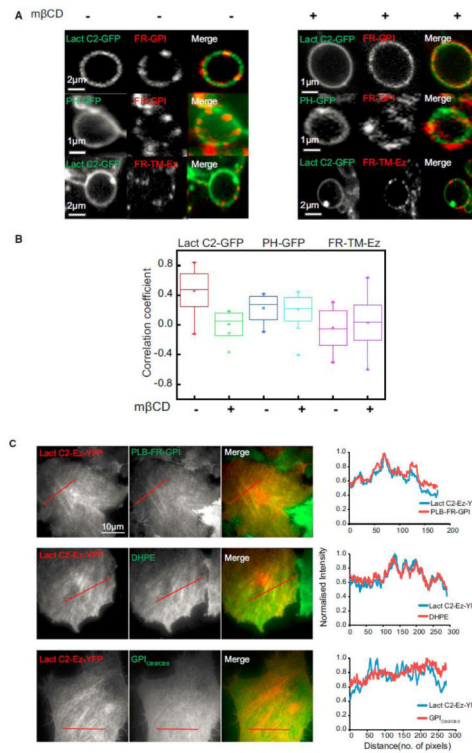


Figure 7.

Crosslinking of Either FR-GPI at the Outer Leaflet or PS at the Inner Leaflet Demonstrates a Strong Transbilayer Coupling (A) Cropped images of membrane blebs obtained after jasplakinolide treatment cells expressing Lact C2 GFP or PH GFP (left, green in merge) either with (treated) or without mbCD (control), followed by cross-linking FR-GPI or FR-TM-Ez (middle, as indicated; red in merge) with primary and secondary antibodies to create micron-sized patches of these proteins. (B) Graph shows the extent of correlation between the intensity fluctuation of crosslinked FR-GPI or FR-TM-Ez and PH GFP or Lact C2 GFP both in the presence (+) and absence (–) of mbCD, determined from images of blebs (pooled from three independent experiments) as shown in (A). (C) Images and normalized line intensity profiles of Lact C2-Ez-YFP transfected in IA2.2 cells labeled with PLB or DHPE or C8 GPI analog as indicated. This shows a strong colocalization in the distribution of Lact C2-Ez-YFP with FR-GPI and DHPE, but not with C8 GPI analog. Red line in (C) depicts the region of line scan measurement. Scale bar, 10 mm. The whiskers represent the outliers. See also Figure S7.